AIP Publishing

This manuscript was accepted by J. Chem. Phys. Click here to see the version of record.

Dissociations of water ions after valence and inner-valence ionization

A. Hult Roos[1], J.H.D. Eland[1,2], J. Andersson[1], R.J. Squibb[1], and R. Feifel[1]

[1]Department of Physics, University of Gothenburg, Origovägen 6B, 412 96 Gothenburg, Sweden

[2]Department of Chemistry, Physical and Theoretical Chemistry Laboratory, Oxford University, South Parks Road, Oxford OX1 3QZ, United Kingdom

Abstract

Energy selected and mass-resolved electron-ion coincidence spectra of heavy water have been recorded for ionization energies from 18 to 35 eV. Dissociation from the B^2B_2 state produces both O^+ and D_2^+ at energies near their thermodynamic thresholds in addition to the known products D^+ and OD^+. Relative yields of O^+, OD^+ and D^+ in the B^2B_2 state breakdown diagram are modulated by the vibrational structure of the B-state population, implying incomplete energy equilibration before fragmentation. Decay from the C-state produces OD^+ in addition to the known O^+ and D^+. The fragment kinetic energies suggest that O^+ and D^+ from the C state are products of full atomization of the molecule.

Introduction

When water molecules are ionized by high energy charged particles or by light with photon energies between 12.6 and 500 eV, H_2O^+ ions are initially formed mainly in the four electronic states, X^2B_1, A^2A_1, B^2B_2 and C^2A_1, with vertical ionization energies of 12.6, 15, 19 and 32 eV above the ground state of neutral water. Although the inner-valence (IV) band centred at 32 eV in the photoelectron spectrum is not well described as a single state, it is convenient to refer to it as if it were. In this paper the ionization band between 30 and 35 eV is called the C-state, to distinguish it from ionization to less strongly populated IV states at higher and lower energy. The four main states arise predominantly by single electron removal from the four outer orbitals in the electron configuration of the neutral molecule:

$$1a_1^2\ 2a_1^2\ 1b_2^2\ 3a_1^2\ 1b_1^2\ .....X^1A_1$$

The energies and spectra of water ions in their ionized states have been studied for nearly a century; wide-ranged and detailed information on the lower energy states came first from photoelectron spectroscopy [1-5] and threshold photoelectron spectroscopy [6] together with optical emission studies [7-9] and theoretical calculations [10-15]. Fine spectroscopic detail of the A – X transition has come more recently from the absorption spectrum measured by optical heterodyne magnetic rotation enhanced velocity modulation spectroscopy [16]. In the X and A states, as populated by vertical transitions from the ground-state neutral molecule, the molecular ions remain intact as H_2O^+, and A → X optical emission is observed with lifetimes of the order of 10 μs [17]. The lowest few vibrational levels of the B-state also survive as intact molecular ions, but no emission has been detected from them although a dipole transition to the A state is optically allowed. The lifetimes of these metastable levels within the B state have recently been measured as 198 ± 11 μs [18]. The higher levels of B and the whole populated range of the C-state are fully (pre)dissociated. The fragmentation pathways and dynamics of B-state dissociation have been studied by photoionization

ACCEPTED MANUSCRIPT

AIP Publishing

This manuscript was accepted by J. Chem. Phys. Click here to see the version of record.

mass spectrometry [19-21], photoelectron-photoion coincidence (PEPICO) [22,23] and threshold photoelectron-photoion coincidence (T-PEPICO) [24], while decay from the C-state has been examined by photoionization mass spectrometry [21] and electron-impact coincidence simulation [25].

In this work we re-examine the dissociations of water ions from the B- and C-states by the relatively new technique of magnetic-bottle photoelectron-photoion coincidence, achieving better statistics and signal-to-noise ratios than previous studies. This allows us to delineate minor pathways in the B-state decay that have not been observed before, to cast light on the question of whether internal vibrational energy is fully equilibrated before decay from that state [5, 24], and to examine decays from the C-state much more comprehensively than before. To reduce the demands on mass resolution for the ion spectrometer, deuterated water was used in this study. Despite the mass difference, the dissociation mechanisms are considered to be essentially the same for deutereated and undeuterated water, as clearly seen in previous works where undeuterated and deuterated water were compared [5, 24]. The TPES photoionization yields for H_2O and D_2O in the energy region relevant for this study are given by the work of Stockbauer [39], and the photoionization yields for H_2O and D_2O are given by Dehmer and Holland [40].

The dynamics of predissociation from the B state have been discussed theoretically several times [26-30] since the original analysis by Fiquet-Fayard and Guyon [26], who pointed out that since B^2B_2 does not correlate directly to ground state fragments, production of both $OH^+ + H$ and $H^+ + OH$ must be predissociations involving transition to other potential energy surfaces. The mechanisms for formation of OH^+ and H^+ are now considered to involve transfer of most of the initial B-state population to the A-state through a conical intersection at small (ca. 70^o) HOH angle. This very rapid transfer accounts for diffuseness in the photoelectron spectrum. The A-state can dissociate to ground-state $H^+ + OH$, to which it correlates adiabatically. Ground-state $OH^+ + H$ can be formed by spin-orbit coupling-mediated transfer from A (or B) to a quartet state (a^4B_1 in C_{2v}, a^4A'' in C_s) at other conical intersections. A further transition from A to X, mediated by Renner-Teller coupling, provides another path to ground-state $OH^+ + H$, because X correlates directly to these products. The A- and X-states become degenerate in the linear configuration, so this path presumably involves a big excursion in bond angle. Both H^+ and OH^+ appear as ground-state products, that is, at their lowest thermodynamically possible ionization energies. From the first dynamical calculations of Lorquet and Lorquet [38], through extended treatments by Dehareng et al. [27, 28], to the wavepacket propagation calculations of Reutt et al. [5] and most recently those of Suárez et al. [30], it has become increasingly clear that to account for the observed characteristics of decay from the H_2O^+ B state, a model including at least both A- and X- states' involvement is necessary. The conclusion that the first step in OH^+ formation from B is population transfer to A is further supported by the detailed velocity-map imaging experiments and accompanying potential energy surface calculations by Sage et al. [29]. The most complete modelling of the B-state decay up to now is the study of wavepacket propagation on highly correlated potential energy surfaces by Suárez et al. [30], which treats the behaviour of the whole electronic state as populated by initial vertical ionisation to B. The overall branching from B to the main products in model calculations, which require only the doublet states, agrees with the experimental branching ratios of Tan et al. [25]. Some particular predictions [29] are that redistribution of almost the whole population from B to A occurs within 10 fs, X is populated after about 50 fs and product OH^+ and H^+, predominantly in their ground states, are formed on a 100 fs to 10 ps time scale. These predictions are currently subjects of experimental investigation at the fs VUV-FEL facility FERMI by the methods recently pioneered there by Squibb et al. [31]. In contrast to

ACCEPTED MANUSCRIPT

AIP Publishing

This manuscript was accepted by J. Chem. Phys. Click here to see the version of record.

this wealth of work on the B-state, dissociation specifically from the C^2A_1 state of H_2O^+ has been examined before only by the electron-impact-simulated photoionization experiments of Tan et al. [25], and to the best of our knowledge, no theoretical treatment of it exists.

Experimental

As in some earlier work, D_2O was used in preference to H_2O to reduce the experimental demands on ion mass resolution. Ionization of D_2O molecules in an effusive jet was by wavelength-selected light from a fast pulsed capillary discharge in He. The apparatus combines a magnetic bottle time-of-flight (TOF) electron spectrometer with a collinear TOF ion mass analyser in the configuration originally developed and described by some of us [32], with only minor modifications as shown in Fig. 1. Energy-selected electrons and mass-selected ions are recorded continuously, with no effective limit on the number of electrons or ions in each event. Briefly, the electronically switched pulsed discharge lamp with He working gas produces He resonance light at a repetition rate of 4.5 kHz in pulses of 2-5 ns duration, followed by a weak afterglow starting about 200 ns later and persisting for up to 10 µs. A toroidal grating monochromator selects individual He I or He II lines to ionise target D_2O gas in an effusive jet emanating from a fine needle. The ionization region is kept electric-field free for 150 ns after the light pulse, to allow all electrons of interest to be directed by the strong and divergent field of a ring magnet with a hollow conical soft-iron pole piece through an earthed grid and into the 2.2 m long flight tube where a weak solenoid field reigns. Electrons are registered as signals from a multichannel plate detector at the far end of the solenoid.

After the initial 150 ns delay the source field is driven to ca. 120 Vcm^{-1} by a 2 µs pulse to propel ions into a two stage time-of-flight mass spectrometer. In the present experiments mass resolution for thermal ions was about 1 in 25 (FWHM) while electron energy resolution was about 5%. The overall collection + detection efficiencies for ions and electrons were about 25 % and 30 % respectively. The efficiency has the same value for D^+ ions with less than 1.5 eV initial kinetic energy and for all the heavier ions, but for D^+ ions with higher initial energy there may be losses which cannot be quantified at present as they depend on the unknown angular distributions. All timing data was collected using a multi-hit time-to digital converter based in a personal computer. The base pressure in the apparatus with no sample was about 1 x 10^{-7} mbar; runs were done at pressures in the main chamber ranging from 9 x 10^{-7} mbar to 6 x 10^{-6} mbar.

ACCEPTED MANUSCRIPT

AIP Publishing

This manuscript was accepted by J. Chem. Phys. Click here to see the version of record.

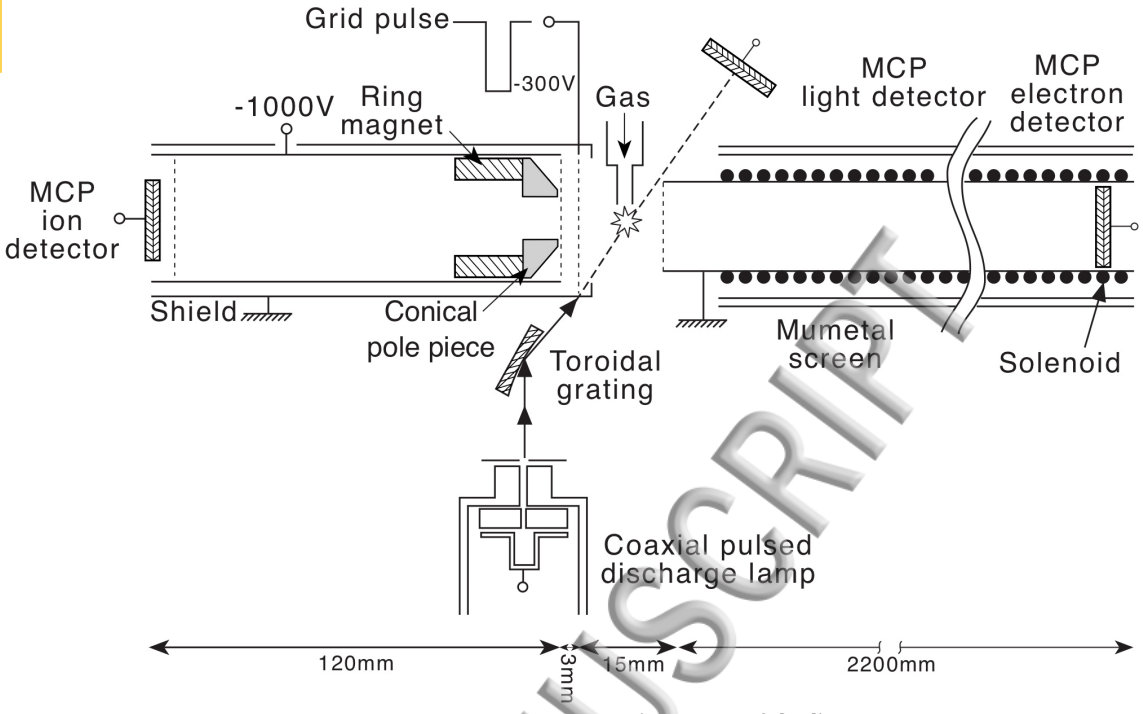

Figure 1. The photoelectron-photoion coincidence apparatus (see also Ref. [32]).

Measurements were carried out at two photon energies, 21.22 and 23.08 eV for studies of B-state dissociation and at two higher energies, 40.81 and 48.37 eV for examination of the C-state. The target gas pressure was varied systematically to quantify and eliminate interfering signals from accidental coincidences and two-body processes, as explained below. Retarding potentials of 1 or 2 V on the electron flight tube were applied in some runs to improve energy resolution for the B-state. Run times of 12 to 48 h were used to gather data from up to 2 x 10^6 ionization events at each pressure and photon energy.

D_2O of purity 99.9 atom % was bought as a commercial product (Sigma Aldrich), but even after a period of conditioning the apparatus with fresh samples, the mass spectra still showed traces (< 3%) of HDO. The HDO^+, OH^+ and H^+ ions are mass resolved and cannot affect the results in any way, while OD^+ from the small proportion of HDO would have negligible effect. If there is sufficient hydrogen exchange that D_2O, HDO and H_2O are in equilibrium there should be essentially no H_2O^+ at m/q = 18 to be confused with the OD^+ signals.

Data reduction and treatment of unwanted (false) coincidences

Apart from the usual accidental coincidences, which are present in all multi-particle coincidence experiments and are relatively easily allowed for as explained below, data taken by the present technique suffer from some other sources of real but unwanted coincidences. First, the pulsed helium discharge lamp emits a weak afterglow on all the useful ionizing lines, starting a few hundred ns after the main pulse and continuing for several μs. The intensity profile of this afterglow depends on the precise lamp conditions (He pressure, He purity, lamp history) and is different on the different spectral lines, so its effect must be allowed for individually in each experimental run. Its peak intensity is no more than a few percent of that of the main pulse. To determine the profile of the afterglow we examine an electron-ion coincidence signal for parent ions which dissociate completely from excited electronic states and so cannot be formed legitimately with electrons at the

ACCEPTED MANUSCRIPT

AIP Publishing

This manuscript was accepted by J. Chem. Phys. Click here to see the version of record.

long flight times (low electron energies) corresponding to the afterglow timing. When other effects have been eliminated the D_2O^+- electron coincidence signal fulfils this role in the present experiments.

Secondly, when the photon energy exceeds twice the first ionization energy of a molecule, primary photoelectrons from one event may ionize a second molecule by electron impact, releasing two electrons with lower energy and a continuous energy distribution. This phenomenon is quite general in photoionization though not always recognized; its intensity is proportional to the square of the target gas pressure and here it can occur only with the higher energy (40.81 and 48.37 eV) photon lines. It can be identified unambiguously by the production of coincident electron pairs with summed energy too high for double ionization of a single molecule. In measurements on D_2O at a chamber pressure of 2.6 x 10^{-6} mbar electron pairs coincident with D_2O^+, OD^+ and D^+ ions were detected with significant intensity and with apparent double ionization energy thresholds exactly matching the two-molecule threshold energies (25.2 eV for D_2O^+, 30.7 eV for OD^+ and 31.3 eV for D^+). This effect was reduced to negligible intensity at a chamber pressure of 9 x 10^{-7} mbar, used in all later experiments at the higher photon energies. Finally, the well-known ion-molecule reaction

$$D_2O^+ + D_2O \rightarrow D_3O^+ + OD$$

could be detected as a clear D_3O^+ signal in the coincident mass spectra at all photon energies. Its quadratic pressure dependence was verified, and as the products of this reaction do not overlap with any of the product ions of interest in this work it does not interfere. Other ion-molecule reactions such as

$$OD^+ + D_2O \rightarrow D_2O^+ + OD$$

or

$$OD^+ + D_2O \rightarrow D_3O^+ + O$$

are known [33] and could possibly interfere by depleting products of interest, but we believe that their effect is negligible at the low pressures finally used.

The data from these experiments consist of counts of electrons and ions from individual detected events in time bins of equal width. To facilitate error analysis and accidental coincidence removal, most of the data reduction is carried out in this time domain, with conversion to energies or ion masses as the final step. This strategy is important because it is only in the time domain that the widths of ion mass peaks and the shapes of islands in coincidence maps can be directly related to the correlated momenta of the ions and hence to kinetic energy releases. The primary data are two-parameter coincidence maps of ion TOF versus electron TOF. For accidental coincidence subtraction, artificial maps with identical dimensions are created as products of the total detected electron and ion spectra, divided by the total number of events, for subtraction from the experimental maps. This procedure is equivalent to covariance analysis for the low event rates used in this work (see, e.g., Ref. [34] and refs. therein). The normalisation sometimes needs slight adjustment to ensure that counts from physically impossible electron-ion combinations are correctly subtracted within the uncertainty set by the counting statistics. At the low event rates used in this work the subtraction has only a very minor effect on the intensities of decays from the B state, whose photoelectron signal and true coincidence rate are far above background. It is more important in examination of decays from the C state, whose photoelectron signal is much weaker at both of the higher (He II) photon energies used.

ACCEPTED MANUSCRIPT

This manuscript was accepted by J. Chem. Phys. Click here to see the version of record.

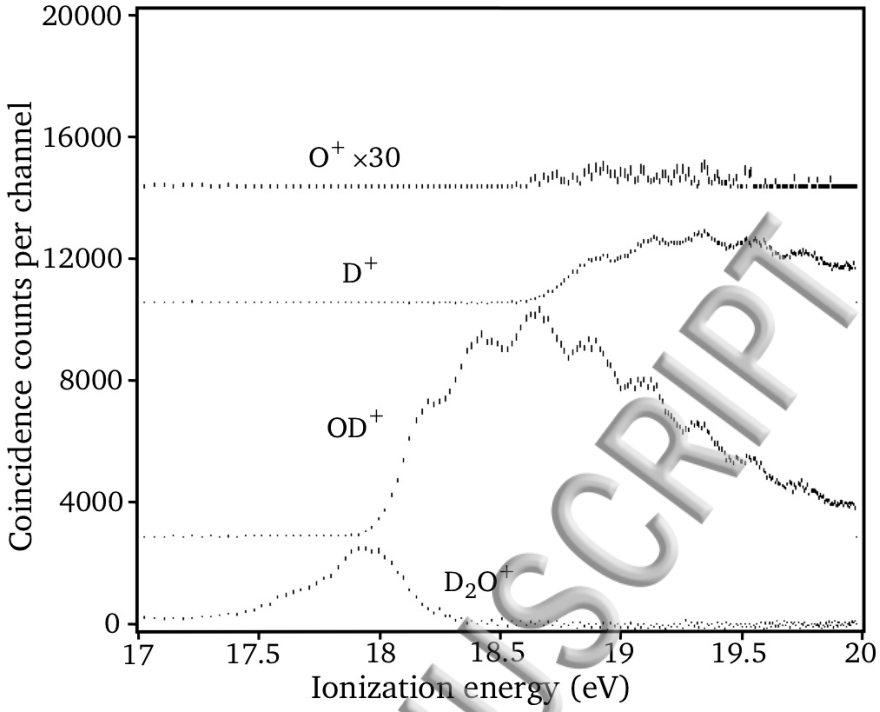

Figure 2. Photoelectron spectra coincident with product ions over the energy range of the B^2B_2 state of D_2O^+, taken at 21.22 eV photon energy with 1 eV retardation of the electrons to improve resolution. Accidental coincidences have been subtracted and incorporated in the 2σ error bars. The data are on a common intensity scale with vertical offsets and amplification of x30 for the O^+ signals.

Results and discussion

Decays from the B^2B_2 state.

Population of the B state of D_2O^+ by photoionization of the neutral molecule covers the energy range from 17.3 to 20.5 eV, encompassing the 0 K thresholds for formation of OD^+ ($X^3\Sigma^-$) 18.07 eV, $D^+ + OD(X^2\Pi)$ 18.67 eV and O^+ (^4S) + D_2 18.71 eV [24]. The thresholds for OD^+ ($a^1\Delta$) 20.26 eV [41], OD^+ ($A^3\Pi$) 21.6 eV [42] and $D_2^+ + O(^3P)$ 20.61 eV [43] are above the main B-state range, but may be reached in the extended tail of the band on the high energy side. Mass-resolved photoelectron spectra taken at 21.22 eV photon energy and covering the main range are shown in Fig. 2, where it can be seen that in addition to the major fragments, O^+ ions also appear at or very near to the thermodynamic threshold. The O^+ signal is clear but very weak, in agreement with its intensity in the photoionization mass spectrometric data of Kronebusch and Berkowitz [21]. All the ion signals show intensity modulation as a function of energy, corresponding to the vibrational structure of the B-state band as seen with our limited electron energy resolution. According to the analysis of Reutt et al. [5] one component of the modulation is a progression in the symmetric stretching vibration ν_1, with the peak near 18.5 eV attributable to $v_1 = 4$. In measurements at 23.08 eV and at the higher photon energies we also detect a very weak D_2^+ signal, again appearing at about its thermodynamic threshold.

The relative intensities of different products from the B-state as a whole at 21.22 eV are slightly different from those measured at higher photon energies; products with higher appearance energies appear to be disfavoured by the closeness of the photon energy to the respective

ACCEPTED MANUSCRIPT

AIP Publishing

This manuscript was accepted by J. Chem. Phys. Click here to see the version of record.

dissociation limit of the fragments. At photon energies of 23.08 eV, 40.81 eV and 48.37 eV, the relative intensities of product ions from B are consistently:

D_2O^+ 10 ± 2 %, OD^+ 70 ± 3 %, D^+ 19 ± 2 %, O^+ 0.15 ± .05 %, and D_2^+ 0.1 ± .05 %.

These proportions of the major products are in good agreement with the values for B-state dissociation in undeuterated H_2O^+ from the electron-impact simulated photoionisation results of Tan et al. [25] and thus also with the wavepacket calculations of Suárez et al. [30]. A breakdown diagram derived from the same data as Fig. 2 is shown as Fig. 3.

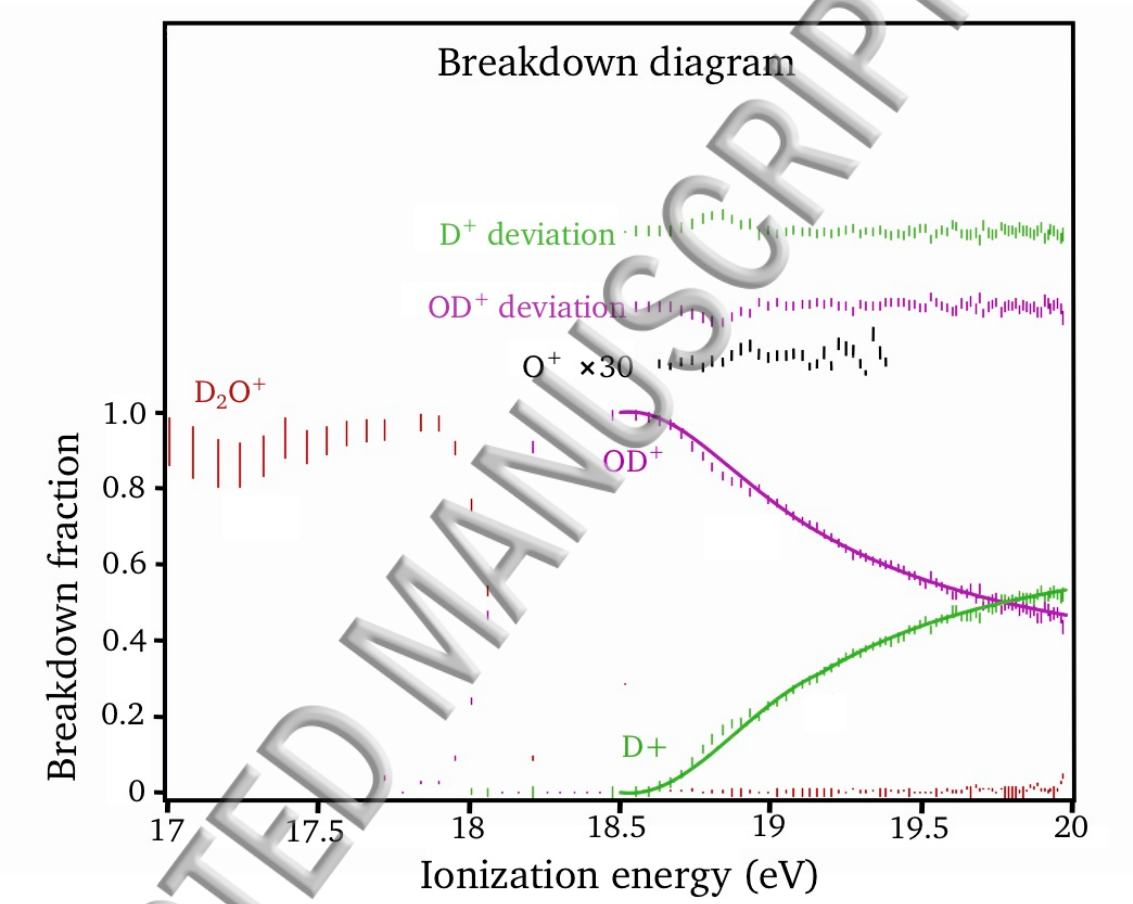

Figure 3. Breakdown diagram derived from the data of Fig. 2. The breakdown fractions for D^+ and OD^+ are compared with the smooth curves shown as continuous lines, derived as explained in the text. The deviations are shown above.

The overall shape of the breakdown diagram, Fig. 3, derived from the mass-resolved photoelectron spectra is the same as that of previous versions from different investigators [22-24] with only minor differences; most importantly, the statistics are substantially improved, so that the real existence of modulation in the breakdown curves for OD^+, D^+ and O^+ cannot be denied. The experimental curves for D^+ and OD^+ are contrasted in the figure with smooth curves generated using the simplest form of RRK (Rice-Ramsperger-Kassel) theory [35] for the rate constants k_j for competing unimolecular dissociations with threshold energy E_{0j} at total energy E:

$$k_j = R_j (1 - E_{0j}/E)^s$$

ACCEPTED MANUSCRIPT

AIP Publishing

This manuscript was accepted by J. Chem. Phys. Click here to see the version of record.

Here R_j is a characteristic rate constant for each reaction and s is an effective number of oscillators (classically one less than the number of vibrational modes). A very good fit to the observed curves is obtained with $R_D = 3R_{OD}$ and s = 2.8. The absolute values of the characteristic rate constants R_j and of the total energy E do not affect the breakdown fractions, so nothing can be deduced from the goodness of fit about the rates or identity of the operative electronic state. The clearest features to emerge from the comparison are a peak relative to the smooth curves for D^+ and a complementary dip for OD^+ at 18.8 eV. The much weaker breakdown curve for O^+ has a peak at 18.9 eV. The same modulation relative to monotonic curves is visible in the breakdown diagram of Norwood et al. [24] for OD^+ and D^+ at exactly the same energy (659 Å). A secondary feature is just discernible at 19.25 eV as another peak for D^+ and complementary dip for OD^+. The existence of this modulation means that internal vibrational energy is not fully equilibrated within the B-state before its decay, as already suspected by Reutt at al. [5] from detailed analysis of the well-resolved photoelectron spectrum. This is hardly surprising if the 10 fs lifetime of B before transfer to A, as calculated by Suárez et al. [30] is correct, since the dwell time in the B-state is then too short for complete internal vibrational redistribution. For comparison, the highest frequency vibration in neutral D_2O has a period of 1.2 ps. The implication is that when the A-state is reached by transfer from B the molecular geometry is still close to that of the ground state neutral molecule, corresponding to high excitation of the bending vibration in particular. This excitation, possibly accessing linearity, may be expected to favour further conversion from A to X, which is correlated to the process producing OH^+ rather than H^+ [24, 28]. It would seem reasonable for the depth of modulation for O^+ production to be greater than for D^+, since formation of D_2 as the co-product must require access to a restricted part of the vibrational phase space with small D-O-D bond angle, as well as spin-orbit coupling to a quartet surface. The phase of the modulation might also be similar for O^+ and D^+ but opposite for OD^+ if the pathway to O^+ and some part of a pathway to D^+ share a common or neighbouring bottleneck, broached effectively in a specific part of the vibronic manifold. The measurements are consistent with both of these speculations, but error bars are too wide to present them as firm conclusions. An alternative explanation consistent with the observations could be that common feature of O^+ and D^+ formation, in contrast to that of OD^+, stem from the fact that that neither requires access to the X-state.

The kinetic energies released in the main dissociations of water ions from the B state were measured as functions of the ionisation energy by Eland [20] and by Powis and Reynolds [23], and we can only confirm that the energies from TOF peak widths in the present data, which are less precise, are consistent with these earlier measurements. For later comparison we note that approximately one third of the available excess energy is released as translational energy in both OD^+ and D^+ formation.

Decays from the C^2A_1 state

According to Tan et al. [25] the C state of H_2O^+ dissociates only to O^+ and H^+, but here we find that D_2O^+ ions in that state dissociate to a considerable extent to OD^+ as well as to D^+ and O^+. It seems highly unlikely that such different behaviour could be due to isotopic substitution. We suspect instead that it is connected to our observation that all the OD^+ ions formed from $D_2O^+(C)$ have high kinetic energies, as must be expected in view of the high available excess energies available for forming ground-state singly-charged products (ca 9-14 eV, all channels). OH^+ ions with similar high kinetic energy are also formed by ionization to levels above the main C-state region, as

ACCEPTED MANUSCRIPT

AIP Publishing

This manuscript was accepted by J. Chem. Phys. Click here to see the version of record.

demonstrated by the coincidence results of Sann et al. [36]. In that case the ions are formed with a kinetic energy release of 5 eV by indirect double ionisation as $OH^+ + H^+$ ground-state pairs, a process which is energetically impossible below an energy of 31.7 + 5 = 36.7 eV. Because of the high kinetic energy releases, some D^+ and OD^+ ions may go undetected in our experiments, so our estimates of their relative intensities have a degree of uncertainty. There is additional uncertainty from the need to correct the rather weak OD^+ ion signal for overlap from B-state decay carried over by the lamp's afterglow, as mentioned in the section on data reduction. Our best estimates of the overall dissociation branching from the C state of D_2O^+ treated as single ionization are OD^+ 16 %, O^+ 24 % and D^+ 60 %. No D_2^+ is detected from C and we can set an upper limit of 0.4 % on its relative abundance. Our relative intensity ratio of D^+ to OD^+ of 2.5 is similar to the H^+/OH^+ ratio of 2.8 of Tan et al. [25].

The kinetic energies of the three ions formed by dissociation from the C state do not vary perceptibly with ionization energy within the 31 - 34 eV range. From the peak widths, after subtraction of accidental coincidences and effects of the lamp afterglow, we find the kinetic energies of the individual ions to be 3.4 eV for D^+, 0.3 eV for O^+ and 0.5 eV for OD^+. From the shapes of the time-of-flight peaks it appears that D^+ and O^+ ions have broad kinetic energy release distributions, but the distribution is relatively sharp for OD^+. Of the three reactions, only the formation of OD^+ is definitely a two-body dissociation. To estimate the centre-of-mass (CM) energy releases we can nevertheless treat the other two reactions as if they also involved two fragments, because the mass ratio between light and heavy moieties is roughly the same for all reasonable reaction paths. By "reasonable" we mean that paths where an unobserved neutral D atom takes most of the translational energy are excluded. The resulting estimated CM kinetic energy releases, which can be considered as lower limits because of the exclusions, are listed in Table 1.

Table 1. Dissociations from the C^2A_1 state of D_2O^+ near 32 eV

Ion	Relative abundance	CM KER	Maximum available energy
D^+	60 %	4 eV	13.5 eV (2-body), 9 eV (3-body)
O^+	24 %	3 eV	13.3 eV (2-body), 9 eV (3-body)
OD^+	16 %	5 eV	14 eV

Table 1 also lists the maximum available energies for each reaction starting in the C-state at 32 ± 2 eV, assuming that only electronic ground state products are formed. All the heavy fragments also have energetically accessible excited electronic states (O at 2.0 and 4.2 eV, O^+ at 3.3 and 5.0 eV, OD at 4 and 8.5 eV and OD^+ at 2.2 and 3.5 eV), whose formation would reduce the energy available for translation. By analogy with the B-state decay, where about one third of the available energy goes into translation, we conclude that the kinetic energies are most consistent with formation of both D^+ and O^+ as ground state 3-body fragments, and with formation of OD^+ also in its ground electronic state with neutral D. The complete lack of D_2^+ as a competing product also indicates that O^+ is not formed as a partner of molecular D_2. Excited state fragments may be formed, and probably contribute to the kinetic energy release distributions. Double ionisation from the main C-state itself is ruled out on energy grounds; the indirect double ionisation that both we and Sann et al. [36] observe is due to higher excited states. The C state band in the spectrum of water ions represents an inner-valence state which, like its congeners in other molecules is much more complex than a single electron configuration. According to the most detailed SAC-CI (symmetry adapted cluster

ACCEPTED MANUSCRIPT

AIP Publishing

This manuscript was accepted by J. Chem. Phys. Click here to see the version of record.

configuration interaction) calculations of Ning et al. [37] there are as many as 10 states of $^2A_1$, $^2B_1$ or $^2B_2$ symmetry based on $2a_1^{-1}$ ionisation between 30 and 34 eV ionisation energy. In view of this, a simple analysis of symmetry correlations from bound state to products seems unlikely to provide insight into the exact dissociation mechanisms.

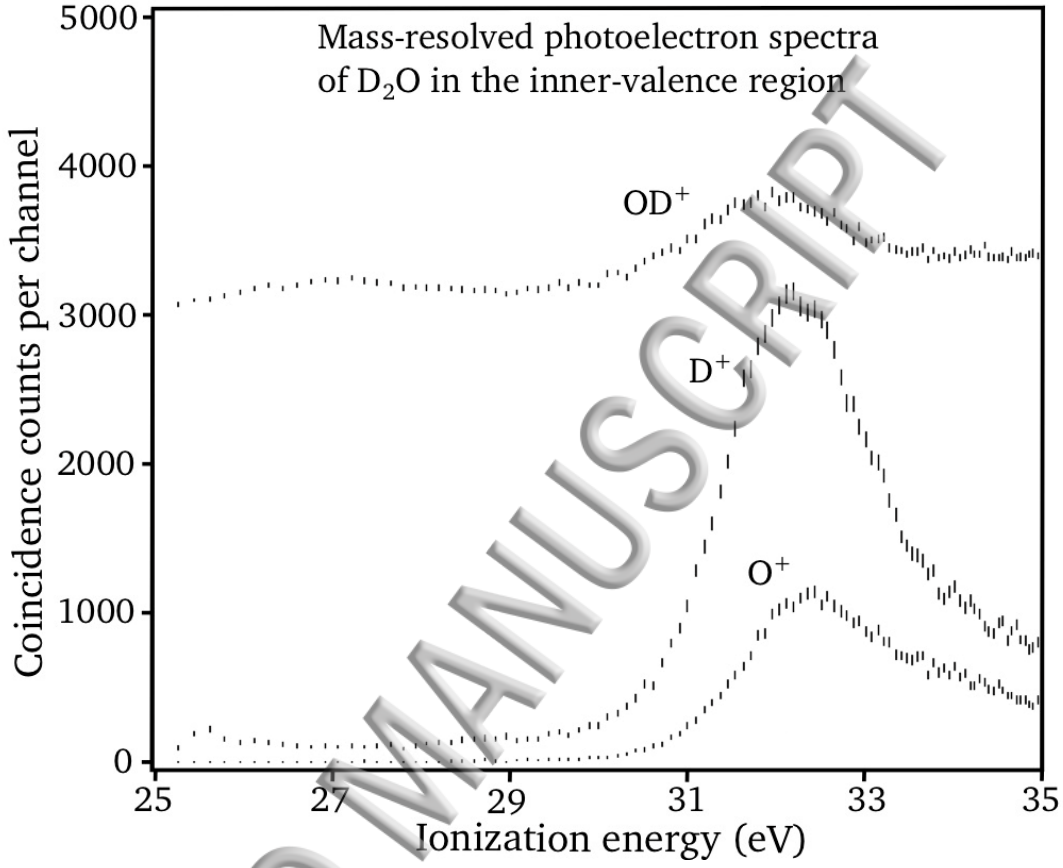

Figure 4. Photoelectron spectra of D_2O at 40.81 eV photon energy coincident with product ions from dissociations in the inner-valence region. The data are on a common intensity scale, with vertical offsets for clarity. The OD^+ data show high kinetic energy ions only, as explained in the text.

Ionization-energy dependences of the different product ion yields from C are shown in Fig. 4. The data for OD^+ is taken from the wings of the time-of-flight peak, which are free from overlap with low-energy OD^+ from B-state decay produced by the lamp afterglow. The cut was made at ±20 ns, which corresponds to an OD^+ energy of about 0.2 eV. Because of this, and also because some high kinetic energy ions may be lost, relative intensities in this figure are less certain than the 2σ error bars might imply. The main observations from these measurements are that D^+, O^+ and OD^+ all appear at essentially the same ionization energies, presumably in competition, and that the "satellite" state at 27 eV appears only in the OD^+ channel. This satellite peak, which also gets its intensity from $2a_1^{-1}$ ionization [37], is seen much more strongly in the threshold photoelectron spectrum [6] than in the regular photoelectron spectra at He II wavelengths or in high-energy electron impact [21, 25, 37]. The kinetic energy of OD^+ from the satellite state is visibly lower than that from the main C-state at 32 eV, but its intensity is too low for a good estimate.

Three-body reactions producing D^+ and O^+ could go by single-step explosions or by sequential two-body steps, where an initial OD or OD^+ dissociates after the first O-D bond breakage. A clue to the mechanism may be given by the momentum correlations in dissociation of water to

ACCEPTED MANUSCRIPT

AIP Publishing

This manuscript was accepted by J. Chem. Phys. Click here to see the version of record.

doubly-charged products, where Sann et al. [36] using the COLTRIMS technique found that a sequential pathway is dominant.

Conclusions

The magnetic bottle photoelectron-photoion coincidence technique applied to the dissociative ionisation of water has yielded mass-selected photoionization spectra and breakdown patterns with improved statistics, allowing minor fragments to be detected. The B^2B_2 state dissociates to both O^+ and D_2^+ with appearance near their thermodynamic thresholds in addition to the known products D^+, OD^+ and D_2O^+. Relative yields of O^+, OD^+ and D^+ in the B-state breakdown diagram are seen to be modulated by vibrational structure of the B-state, implying incomplete energy equilibration before fragmentation. The modulation is almost in-phase for D^+ and O^+, but anti-phase for OD^+, possibly providing a clue to the reaction dynamics for future theory to address. Decay from the C-state produces high kinetic energy OD^+ in addition to the known O^+ and D^+. The fragment kinetic energies and breakdown pattern suggest that O^+ and D^+ from C are products of full atomisation of the molecule.

Acknowledgements

This work has been financially supported by the Swedish Research Council (VR) and the Knut and Alice Wallenberg Foundation, Sweden.

References

[1] M.I. Al-Jobory and D.W. Turner, *J. Chem. Soc.* B 373 (1967).
[2] A.D. Baker, C.R. Brundle and D.W. Turner, *Int. J. Mass Spectrom. Ion Phys*. **1**, 443 (1968).
[3] L. Karlsson et al., *J. Chem. Phys.* **62**,4745 (1975).
[4] R.N. Dixon, G. Duxbury, J.W. Rabalais and L. Åsbrink, *Mol. Phys*. **31**, 423 (1976).
[5] J.E. Reutt, L.S. Wang, Y.T. Lee and D.A. Shirley, *J. Chem. Phys.* **85**, 6928 (1986).
[6] S.Y. Truong et al., *Chem. Phys*. **355**, 183 (2009).
[7] H. Lew and I. Heiber, *J. Chem. Phys.* **58**, 1246 (1973).
[8] H. Lew, *Can. J. Phys.* **54**, 2028 (1976).
[9] S. Leutwyler, D. Klapstein and J.P. Maier, *Chem. Phys.* **74**, 441 (1983).
[10] P.C. Hariharan and J.C. Pople, *Mol. Phys*. **27**, 209 (1974).
[11] J.A. Smith, P. Jorgenson and Y. Öhrn, *J. Chem. Phys.* **62**, 1285 (1975).
[12] G.G. Balint-Kurti and R.N. Yardley, *Chem. Phys. Lett.* **36**, 342 (1975).
[13] P.J. Fortune, B.J. Rosenberg and A.C. Wahl, *J. Chem. Phys.* **65**, 2201 (1976).
[14] C.F. Jackels, *J. Chem. Phys.* **72**, 4873 (1980).
[15] R.A. Rouse, *J. Chem. Phys.* **64**, 1224 (1976).
[16] Y. Gan, X. Yang, Y. Guo, S. Wu, W. Li, L. Yuyan and Y. Chen, *Mol. Phys*. **102**, 611 (2004).
[17] G.R. Möhlmann, K.K. Bhutani, F.J. de Heer and S. Tsurubuchi, *Chem. Phys.* **31**, 273 (1978).
[18] L.S. Harbo, S. Dziarzhytski, C. Domesle, G. Brenner, A. Wolf and H.B. Petersen, *Phys. Rev. A* **89**, 052520 (2014).
[19] V.H. Dibeler, J.A. Walker and H.M. Rosenstock, *J. Res. Natl. Bur. Stand.* **70A**, 459 (1966).
[20] H. Ehrhardt and A. Kreisling, *Z. Naturforschg*. 22a, 2036 (1967).
[21] P.L. Kronebusch and J. Berkowitz, *Int. J. Mass Spectrom. Ion Phys*. **22**, 283 (1976).
[22] J.H.D. Eland, *Chem. Phys.* **11**, 41 (1975).
[23] I. Powis and D.J. Reynolds, *J. Chem. Soc. Faraday Trans.* **87**, 921 (1991).

ACCEPTED MANUSCRIPT

AIP Publishing

This manuscript was accepted by J. Chem. Phys. Click here to see the version of record.

[24] K. Norwood, A. Ali and C.Y. Ng, *J. Chem. Phys.* **95**, 8029 (1991).

[25] K.H. Tan, C.E. Brion, Ph.E. van der Leeuw and M.J. van der Wiel, *Chem. Phys.* **29**, 299 (1978).

[26] F. Fiquet-Fayard and P.M. Guyon, *Mol. Phys.* **11**, 17 (1966).

[27] D. Dehareng, *Chem. Phys*. **110**, 375 (1986).

[28] D. Dehareng, X. Chapuisat, J.C. Lorquet, C. Galloy and G. Rassev, *J. Chem. Phys.* **78**, 1246 (1983).

[29] A.G. Sage, T.A.A. Oliver, R.N. Dixon and M. Ashfold, *Mol. Phys*. **108**, 945 (2010).

[30] J. Suárez, L. Méndez and I Rabadán, *J. Phys. Chem. Lett.*, **6** 72 (2015).

[31] R.J. Squibb et al., *Nature Communications* **9**, 63 (2018).

[32] J.H.D. Eland and R. Feifel, *Chem. Phys.*, **327**, 85 (2006).

[33] W.T. Huntress Jr. and R.F. Pinizotto Jr., *J. Chem. Phys.* **59**, 4742 (1973).

[34] L.J. Frasinski *et al.*, Phys. Rev. Lett. **111**, 073002 (2013).

[35] H.M. Rosenstock, M.B. Wallenstein, A.L. Wahrhaftig and H. Eyring, *Proc. Nat. Acad. Sci. U.S.A.* **38**, 667 (1952).

[36] H. Sann et al., *Phys. Rev. Lett.*, **106**, 133001 (2011).

[37] C.G. Ning, B. Hajgató, Y.R. Huang, S.F. Zhang, K. Liu, Z.H. Luo, S. Knippenberg, J.K. Deng and M.S. Deleuze, *Chem. Phys.* **343**, 19 (2008).

[38] A.J. Lorquet and J.C. Lorquet, *Chem. Phys.* 4, 353 (1974).

[39] R. Stockbauer, *J. Chem. Phys.* **72**, 5277 (1980).

[40] P. M. Dehmer and D. M. P. Holland, *J. Chem. Phys.* **94**, 3302 (1991).

[41] S. Katsumata and D. R. Lloyd, *Chem. Phys. Lett.* **45,** 519 (1977).

[42] A. J. Merer et al., *Can. J. Phys.* **53**, 251 (1975).

[43] B. Ruscic et al., *J. Phys. Chem. A* **108**, 9979 (2004).

ACCEPTED MANUSCRIPT

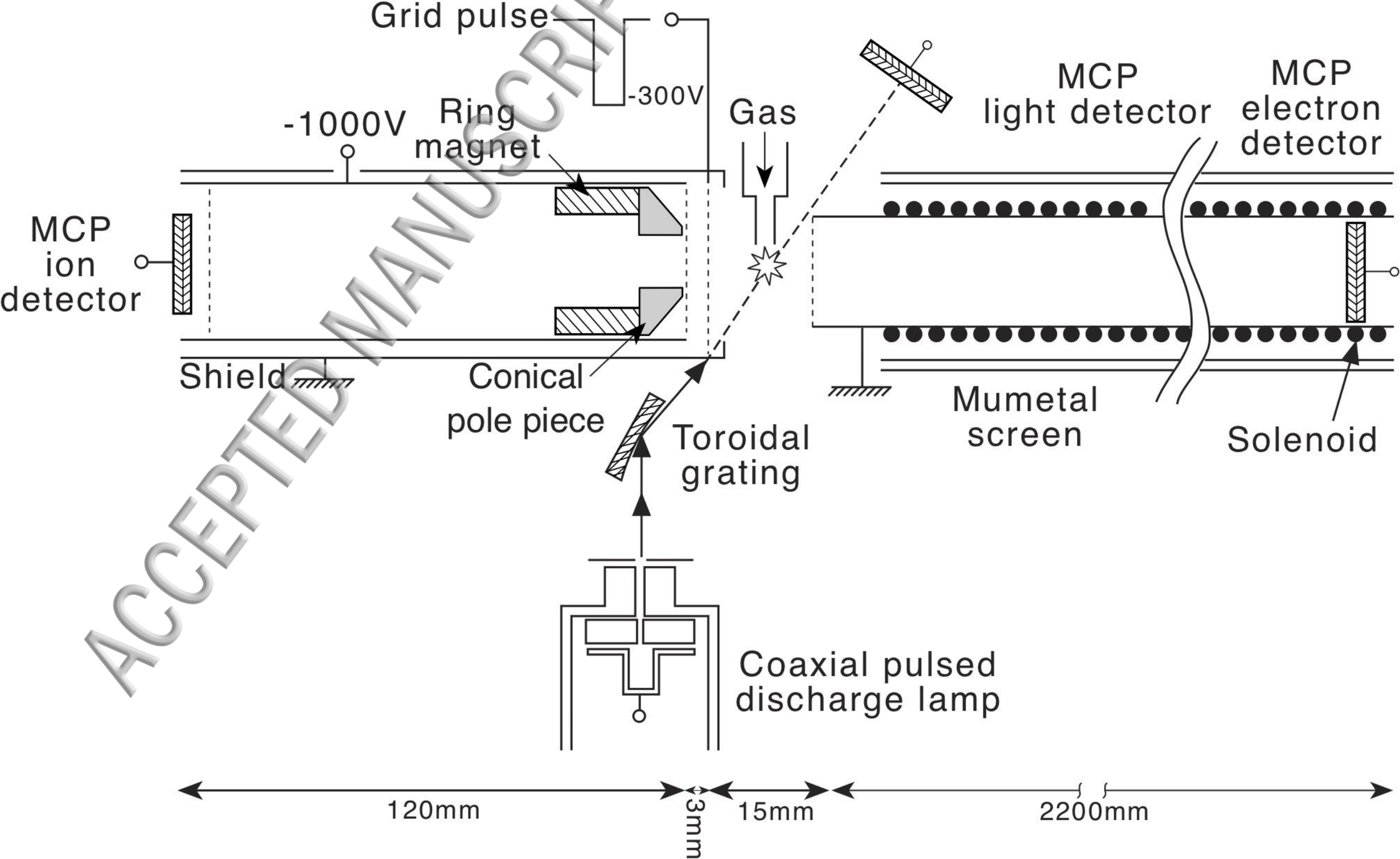

ACCEPTED MANUSCRIPT

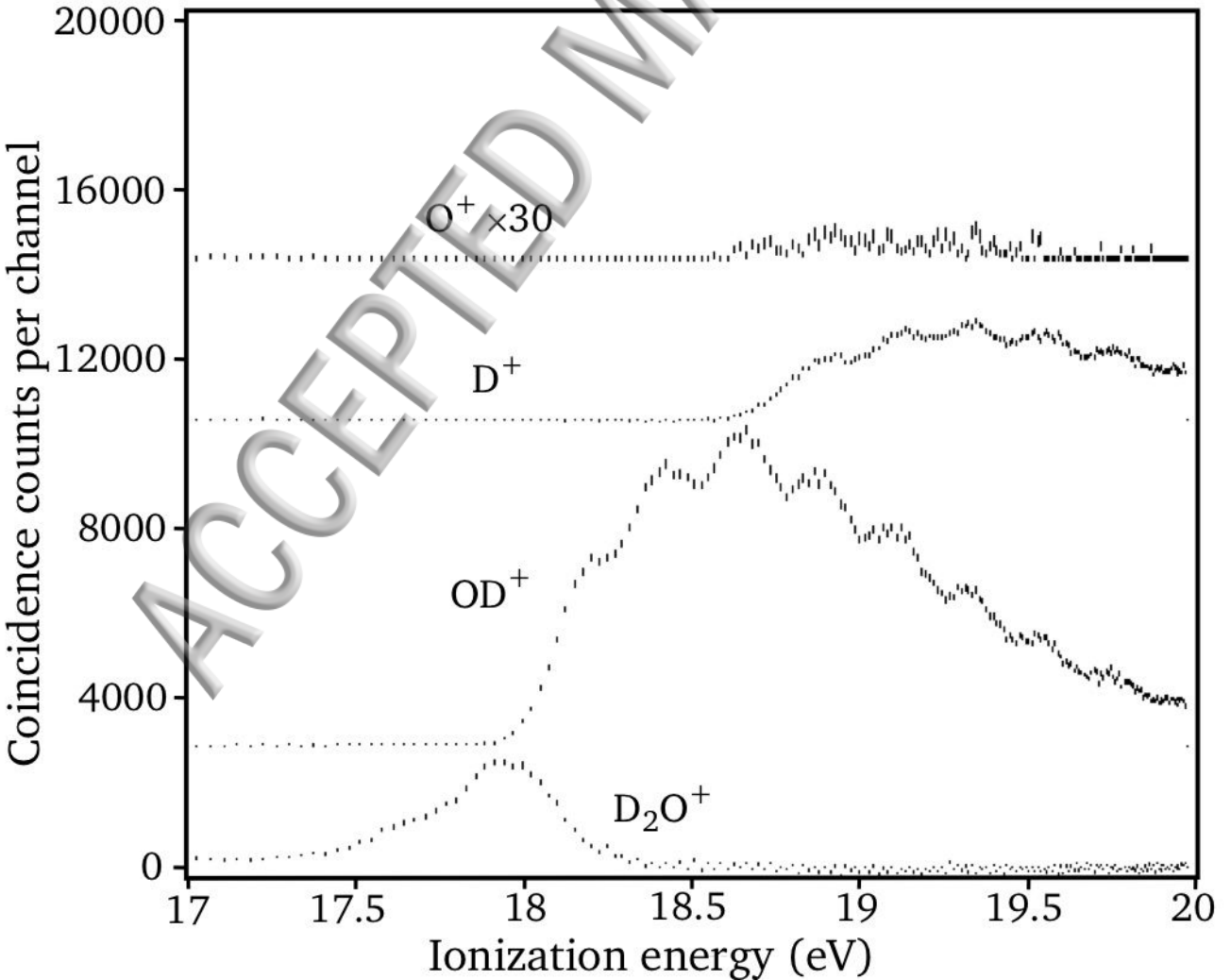
20000
16000
12000
8000
4000
0
Coincidence counts per channel
O+ ×30
D+
OD+
D2O+
17
17.5
18
18.5
19
19.5
20
Ionization energy (eV)
ACCEPTED MA

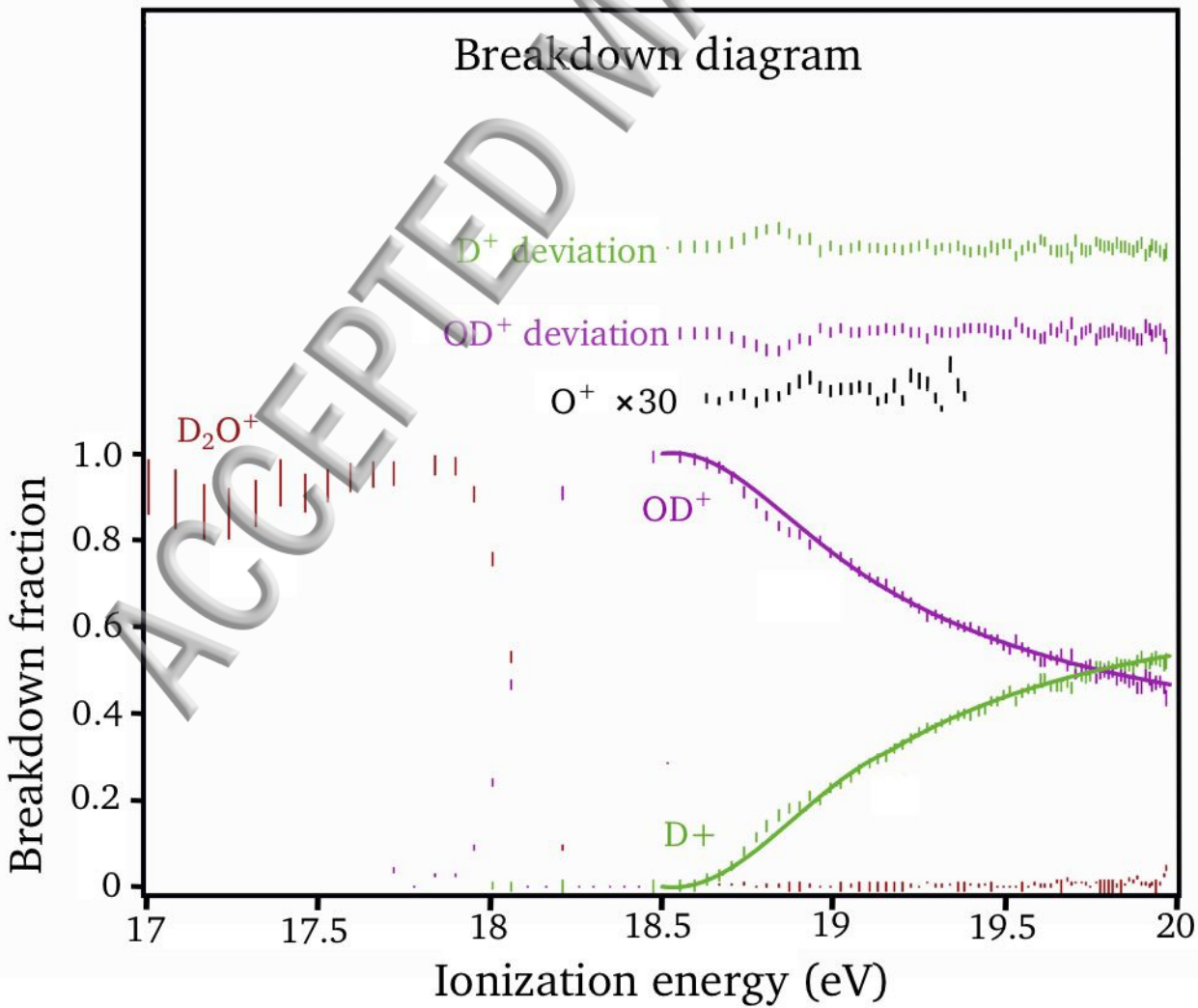
Breakdown diagram
D+ deviation
OD+ deviation
O+ ×30
D2O+
OD+
D+
Breakdown fraction
1.0
0.8
0.6
0.4
0.2
0
17
17.5
18
18.5
19
19.5
20
Ionization energy (eV)
ACCEPTED MA

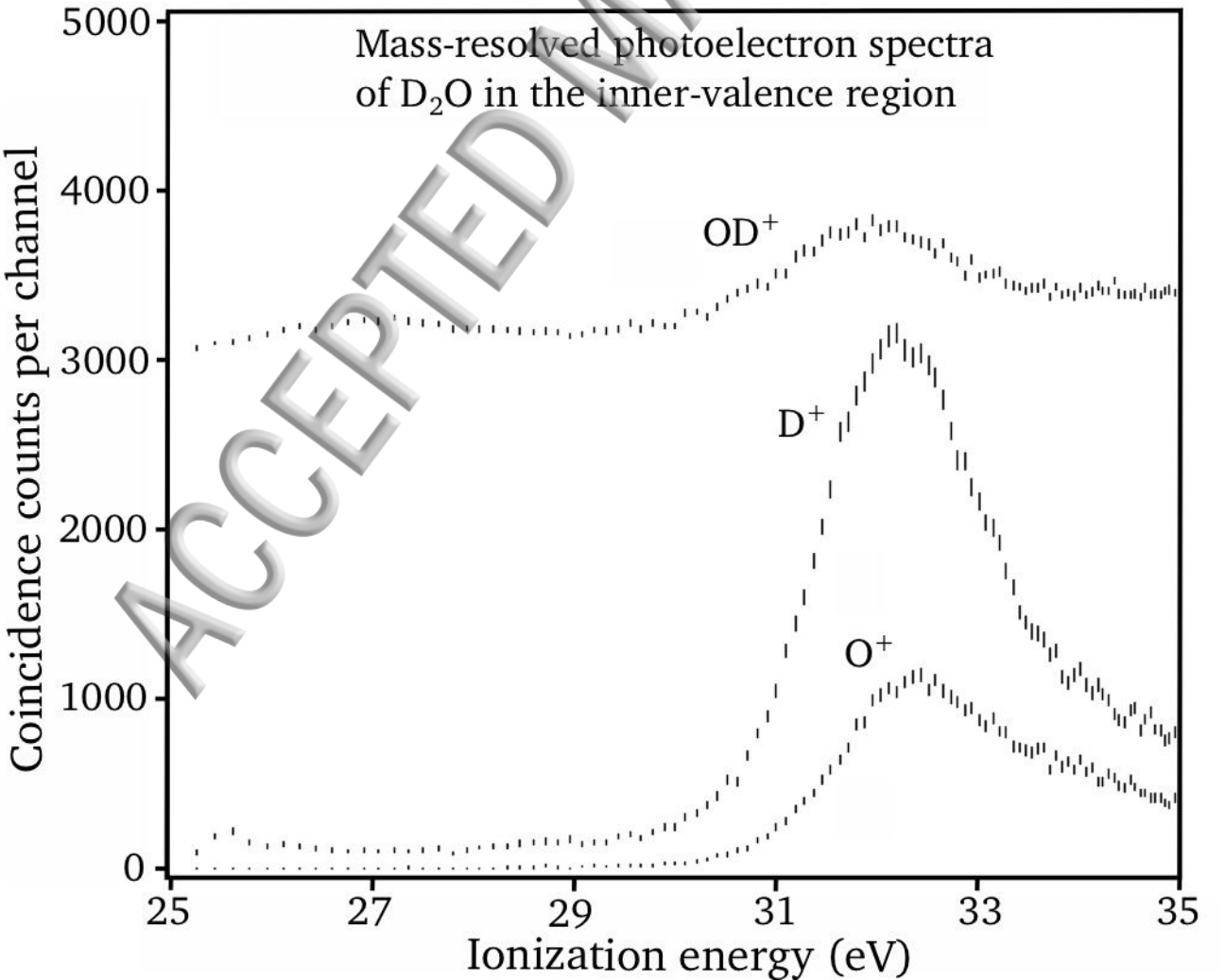
Mass-resolved photoelectron spectra
of D_2O in the inner-valence region
OD^+
D^+
O^+
Coincidence counts per channel
0
1000
2000
3000
4000
5000
25
27
29
31
33
35
Ionization energy (eV)
ACCEPTED MA